



**HAL**  
open science

## A genomic duplication spanning multiple P450s contributes to insecticide resistance in the dengue mosquito *Aedes aegypti*

Tiphaine Bacot, Chloé Haberkorn, Joseph Guilliet, Julien Cattel, Mary Kefi, Louis Nadalin, Jonathan Filee, Frederic Boyer, Thierry Gaude, Frederic Laporte, et al.

► **To cite this version:**

Tiphaine Bacot, Chloé Haberkorn, Joseph Guilliet, Julien Cattel, Mary Kefi, et al.. A genomic duplication spanning multiple P450s contributes to insecticide resistance in the dengue mosquito *Aedes aegypti*. 2024. hal-04745935

**HAL Id: hal-04745935**

**<https://hal.science/hal-04745935v1>**

Preprint submitted on 21 Oct 2024

**HAL** is a multi-disciplinary open access archive for the deposit and dissemination of scientific research documents, whether they are published or not. The documents may come from teaching and research institutions in France or abroad, or from public or private research centers.

L'archive ouverte pluridisciplinaire **HAL**, est destinée au dépôt et à la diffusion de documents scientifiques de niveau recherche, publiés ou non, émanant des établissements d'enseignement et de recherche français ou étrangers, des laboratoires publics ou privés.



Distributed under a Creative Commons Attribution - NonCommercial - NoDerivatives 4.0 International License

## A genomic duplication spanning multiple P450s contributes to insecticide resistance in the dengue mosquito *Aedes aegypti*

Tiphaine Bacot<sup>1</sup>, Chloé Haberkorn<sup>§,1</sup>, Joseph Guilliet<sup>§,1,2</sup>, Julien Cattel<sup>§,1</sup>, Mary Kefi<sup>§,3</sup>, Louis Nadalin<sup>1</sup>, Jonathan Filee<sup>2</sup>, Frederic Boyer<sup>1</sup>, Thierry Gaude<sup>1</sup>, Frederic Laporte<sup>1</sup>, Jordan Tutagata<sup>1</sup>, John Vontas<sup>3,4</sup>, Isabelle Dusfour<sup>5</sup>, Jean-Marc Bonneville<sup>#,1</sup>, Jean-Philippe David<sup>#,1,\*</sup>

# equal contribution

§ equal contribution

\* corresponding author

<sup>1</sup> Laboratoire d'Ecologie Alpine (LECA, UMR 5553), Université Grenoble-Alpes (UGA), Université Savoie Mont-Blanc (USMB), CNRS, 38041 Grenoble, France.

<sup>2</sup> Université Paris-Saclay, CNRS, IRD, UMR Évolution, Génomes, Comportement et Écologie, 91198 Gif-sur-Yvette, France.

<sup>3</sup> Institute of Molecular Biology and Biotechnology, Foundation for Research and Technology Hellas, Heraklion, Greece.

<sup>4</sup> Pesticide Science Laboratory, Department of Crop Science, Agricultural University of Athens, Athens, Greece.

<sup>5</sup> Vectopôle Amazonien Emile Abonnenc, Institut Pasteur de la Guyane, Cayenne, France ; Global Health Department, Institut Pasteur, Paris, France.

\* [jean-philippe.david@univ-grenoble-alpes.fr](mailto:jean-philippe.david@univ-grenoble-alpes.fr)

## Abstract

1 Resistance of mosquitoes to insecticides is one example of rapid adaptation to anthropogenic  
2 selection pressures having a strong impact on human health and activities. Target-site modification  
3 and increased insecticide detoxification are the two main mechanisms underlying insecticide  
4 resistance in mosquitoes. While target-sites mutations are well characterised and often used to track  
5 resistance in the field, the genomic events associated with insecticide detoxification remain partially  
6 characterised. Recent studies evidenced the key role of gene duplications in the over-expression of  
7 detoxification enzymes and their potential use to track metabolic resistance alleles in the field.  
8 However, such genomic events remain difficult to characterise due to their complex genomic  
9 architecture and their co-occurrence with other resistance alleles. In this concern, the present work  
10 investigated the role of a large genomic duplication affecting a cluster of detoxification enzymes in  
11 conferring resistance to the pyrethroid insecticide deltamethrin in the mosquito *Aedes aegypti*.

12 Two isofemale lines originating from French Guiana and being deprived from major target-site  
13 mutations showed distinct insecticide resistance levels. Combining RNA-seq and whole genome pool-  
14 seq identified a 220 Kb genomic duplication enhancing the expression of multiple contiguous  
15 cytochrome P450s in the resistant line. The genomic architecture of the duplicated loci was  
16 elucidated through long read sequencing, evidencing its transposon-mediated evolutionary origin.  
17 The involvement of this P450 duplication in deltamethrin survival was supported by a significant  
18 phenotypic response to the P450 inhibitor piperonyl butoxide together with genotype-phenotype  
19 association and RNA interference. Experimental evolution suggested that this P450 duplication is  
20 associated with a significant fitness cost, potentially affecting its adaptive value in presence of other  
21 resistance alleles.

22 Overall, this study supports the importance of genomic duplications affecting detoxification enzymes  
23 in the rapid adaptation of mosquitoes to insecticides. Deciphering their genomic architecture  
24 provides new insights into the evolutionary processes underlying such rapid adaptation. Such  
25 findings and provides new tools for the surveillance and management of resistance in the field.

26 **Key words:** Mosquito; Insecticide resistance; P450; Gene duplication; Kdr mutation; *Aedes aegypti*

27

## 28 Introduction

29 Natural populations experience a wide range of selective pressures, leading to the accumulation of  
30 locally adaptive features and the expression of complex phenotypes (Orr, 2005). Among them, those  
31 driven by human activities promote novel and strong selective pressures. Understanding the genetic  
32 mechanisms allowing populations to quickly respond to rapid environmental changes has become a  
33 major goal (Hendry et al., 2008, 2017; Palumbi, 2001). Resistance of insects to insecticides is a key  
34 example of rapid evolution under strong anthropogenic selective pressures. This adaptation has  
35 occurred quickly and independently in a large number of taxa with frequent parallel trajectories  
36 (Ffrench-Constant et al., 2004; Liu, 2015). As a consequence of local and temporal variations of the  
37 selection pressures, the genetic modifications affecting resistant populations are often complex and  
38 combine several resistance mechanisms that are potentially additive, each of them bringing variable  
39 fitness costs. In addition, the very strong selection pressure exerted by insecticides is prone to  
40 produce bottleneck effects. Such complexity makes the identification of resistance alleles and the  
41 assessment of their respective contribution challenging (Ffrench-Constant et al., 2004; Li et al., 2007).

42 Besides the understanding of the genetics of rapid adaptation and the origins of complex traits,  
43 deciphering the molecular bases of insecticide resistance is also essential for improving pest  
44 management strategies (Hawkins et al., 2018). Among taxa of major economic and medical  
45 importance, mosquitoes represent a major threat for public health worldwide because of their ability  
46 to transmit human viruses and pathogens (Lounibos, 2002). Among them, *Aedes aegypti* is of  
47 particular importance because of its wide distribution and its capacity to transmit Yellow fever,  
48 Dengue, Zika and Chikungunya viruses (Brown et al., 2014). These arboviruses are now re-emerging  
49 worldwide following the expansion of mosquitoes' distribution area as a consequence of global  
50 warming, global transportation network and land perturbations (Kraemer et al., 2015). Although  
51 efforts are invested in improving vaccine-based prevention strategies (Carvalho & Long, 2021; Garg  
52 et al., 2020; Silva et al., 2018), vector control remains the cornerstone of arboviral diseases control.  
53 However, decades of insecticide usage have led to the selection and spread of insecticide resistance  
54 in this mosquito species, affecting all public health insecticides, including the most-used pyrethroids  
55 (Moyes et al., 2017). High pyrethroid resistance has been shown to reduce vector control efficacy  
56 (Dusfour et al., 2011; Marcombe, Carron, et al., 2009; Marcombe et al., 2011; Valle et al., 2019).  
57 Though greener vector control strategies are being developed, insecticides will likely remain a key  
58 component of integrated vector control in high transmission areas for the next decades (Achee et al.,  
59 2019). In this concern, identifying the genetic factors underlying resistance is crucial for tracking  
60 resistance alleles in the field and making a better use of the few authorised public health insecticides  
61 through resistance management actions (Cattel et al., 2020; Corbel & N'Guessan, 2013; Dusfour et  
62 al., 2019).

63 In mosquitoes, resistance to chemical insecticides is mainly caused by genetic changes decreasing the  
64 affinity of the insecticide for its target (target-site resistance), decreasing its penetration (cuticular  
65 resistance), or increasing its detoxification through complex biochemical pathways (metabolic  
66 resistance) (Li et al., 2007). Pyrethroid insecticides target the neuronal voltage-gated sodium channel  
67 (VGSC gene), and the selection of *knockdown resistance (kdr)* mutations affecting this protein can  
68 lead to resistance. Multiple *kdr* mutations, often combined as haplotypes, have been identified in *Ae.*  
69 *aegypti* with the following ones playing a major role in pyrethroid resistance in South America:  
70 Val410Leu, Val1016Ile and Phe1534Cys (Bregues et al., 2003; Haddi et al., 2017; Hirata et al., 2014;  
71 Kasai et al., 2022; Saavedra-Rodriguez et al., 2007; Smith et al., 2016; Yanola et al., 2011). Today,  
72 these mutations can be tracked in the field using PCR-based diagnostic assays or mass sequencing  
73 approaches, providing essential information for resistance management programmes (Melo Costa et  
74 al., 2020).

75 Conversely, the genetic bases of metabolic resistance are far less understood, though it often  
76 accounts for a significant part of the phenotype (David et al., 2013). Indeed, the complexity and

77 redundancy of xenobiotic biodegradation pathways often lead to multigenic adaptations that can  
78 differ according to the nature and intensity of the selection pressure together with the demographic  
79 and ecological context (Feyereisen et al., 2015; Li et al., 2007). Metabolic resistance to pyrethroids  
80 usually results from an increased activity of detoxification enzymes such as cytochrome P450  
81 monooxygenases (P450s or *CYPs* for genes), glutathione *S*-transferases (GSTs)  
82 carboxy/cholinesterases (CCEs) and UDP-glycosyl-transferases (UDPGTs) (David et al., 2013;  
83 Hemingway et al., 2004; Smith et al., 2016). At the genetic level, this can result from the selection of  
84 enzyme variants showing a higher insecticide metabolism rate, or their overexpression through cis-  
85 or trans- regulation. Genomic duplications can also contribute to overexpression, and duplications  
86 affecting detoxification genes appear frequently associated with insecticide resistance in mosquitoes  
87 (Cattel et al., 2020, 2021; Faucon et al., 2015; Weetman et al., 2018).

88 In addition to the genetic complexity of metabolic resistance alleles, their frequent co-occurrence  
89 with other resistance mechanisms in natural mosquito populations makes them difficult to  
90 characterise. This is the case in French Guiana, where the use of various insecticides, including the  
91 pyrethroid deltamethrin, for decades has led to the selection of highly resistant *Ae. aegypti*  
92 populations combining metabolic resistance alleles and multiple *kdr* mutations such as Val410Leu,  
93 Val1016Ile or Phe1534Cys (Dusfour et al., 2015; Haddi et al., 2017). Although the over-expression of  
94 several detoxification enzymes was supported by both transcriptomics and proteomics (Dusfour et  
95 al., 2015; Epelboin et al., 2021; Faucon et al., 2017), those most contributing to deltamethrin  
96 resistance and the underlying genetic events remain to be identified. A recent study using a  
97 composite population from French Guiana resistant to multiple insecticides identified gene copy  
98 number variations (CNV) as a probable cause of detoxification enzymes overexpression in this region  
99 (Cattel et al., 2020). Through a pool-seq approach targeting >300 candidate genes, this study  
100 identified multiple contiguous P450s from the CYP6 family on chromosome 1 showing an apparent  
101 elevated CNV in association with deltamethrin survival. However, despite the use of controlled  
102 crosses, the multigenic resistance phenotype of this population (carrying the three above-mentioned  
103 *Kdr* mutations at high frequency together with multiple metabolic resistance alleles) did not allow to  
104 conclude about their role in deltamethrin resistance. In addition, the exon-based nature of the  
105 sequencing data generated together with the complexity of *Ae. aegypti* genome did not allow  
106 resolving the genomic architecture of the duplicated locus.

107 In this context, the present study aimed at confirming the contribution of this P450 duplication in the  
108 resistance of *Ae. aegypti* to deltamethrin and at deciphering its genomic architecture. In order to  
109 limit confounding effects from other resistance alleles, two isofemale lines originating from French  
110 Guiana and showing contrasted pyrethroid resistance levels but no apparent resistance to  
111 organophosphate and carbamate insecticides were used (Epelboin et al., 2021). In addition, both  
112 lines lacked the two major *kdr* mutations Val1016Ile and Val410Leu occurring in South America  
113 (Epelboin et al., 2021). Controlled crosses were then used to remove the Phe1534Cys *kdr* mutation  
114 from the resistant line, which retained a P450-mediated resistance phenotype. Then, RNA-seq and  
115 whole genome pool-seq confirmed the presence of a ~200 Kb genomic duplication enhancing the  
116 expression of a cluster of multiple P450 genes in the resistant line. The genomic architecture of the  
117 duplicated loci was elucidated through long read sequencing, providing clues about its evolutionary  
118 origin. Association studies, experimental evolution and reverse genetic were then used to further  
119 investigate the contribution of this duplicated allele to deltamethrin resistance.

120

## 121 Results

122 *Deltamethrin resistance is associated with P450 activity and is autosomal*

123 Two isofemale lines from Ile Royale island (French Guiana) showing contrasted resistance  
124 phenotypes, namely IR03 and IR13 lines, were used as starting material (**Table 1**). Comparative

125 deltamethrin bioassays confirmed that the IR13 line can be categorized as susceptible to  
 126 deltamethrin as previously shown (Epelboin et al. 2021), though its susceptibility was slightly lower  
 127 than the laboratory strain Bora-Bora that was maintained for decades in insectary. Mating IR03  
 128 genotyped individuals allowed producing the IROF line deprived of the three *kdr* mutations majorly  
 129 associated with pyrethroid resistance in South America (*i.e.* Val410Leu, Val1016Ile, Phe1534Cys).  
 130 However, our attempts to remove the only *kdr* mutation remaining, Ile1011Met were not successful  
 131 (see below). Bioassays showed that the IROF line remained highly resistant to deltamethrin with only  
 132 44% mortality to a high dose of insecticide. Mortality levels remains similar between the IR03 and the  
 133 IROF lines suggesting that the removal of the Phe1534Cys *kdr* mutation did not affect the resistance  
 134 phenotype, or was compensated by the retaining of the Ile1011Met *kdr* mutation.

135

136 **Table 1. Origin, resistance status and *kdr* mutations frequencies of the studied lines**

Line	Origin, type	Deltamethrin mortality <sup>1</sup>	Resistance status	f(410Leu) <sub>2</sub>	f(1016Ile) <sub>2</sub>	f(1534Cys) <sub>2</sub>	f(1011Met) <sub>3</sub>
Bora-Bora	Fr. Polynesia, Lab	100	Susceptible	0	0	0	0
IR13	Fr. Guiana, isofemale	95 (91-99)	Susceptible	0	0	0.26	0
IR03	Fr. Guiana, isofemale	43 (26-60)	Resistant	0	0	0.26	0.33
IROF	IR03 cross	44 (34-54)	Resistant	0	0	0	0.50

137 <sup>1</sup> Mortality rates (mean ± SD) previously obtained on 3 days-old females using 0.05% deltamethrin for 40 min (N=10).

138 <sup>2</sup> *kdr* mutation frequencies estimated by qPCR individual genotyping (N=30) and later confirmed by pool-seq whole genome data.

139 <sup>3</sup> *kdr* mutation frequencies estimated from pool-seq whole genome data.

140

141 The involvement of P450s in the resistance phenotype of the IROF line was then confirmed by  
 142 sequentially exposing adult mosquitoes to the P450 inhibitor piperonyl butoxide (PBO) and to the  
 143 insecticide. Such PBO pre-exposure did not significantly affect deltamethrin survival in the  
 144 susceptible IR13 line, but increased mortality by 20% in the IROF line (Wilcoxon test P value = 0.009),  
 145 supporting the contribution of P450-mediated detoxification in the resistance of the IROF line (Figure  
 146 1).

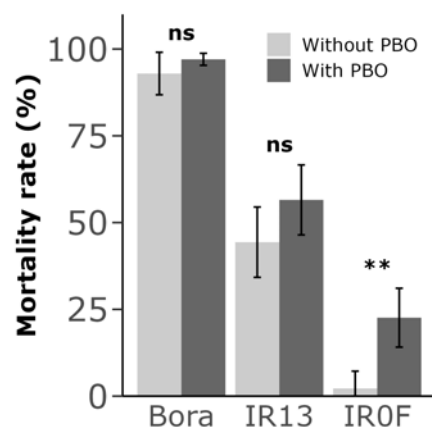


**Figure 1.** Synergistic effect of PBO on deltamethrin resistance. Adult females were exposed or not to 4% PBO for 1h followed by a 30-min exposure to 0.03% deltamethrin. Mortality was recorded 24h after exposure. Mean mortality rates are indicated ± SD, and compared using a Wilcoxon test (N=5, ns: not significant; \*\*: p-value < 0.01).

157

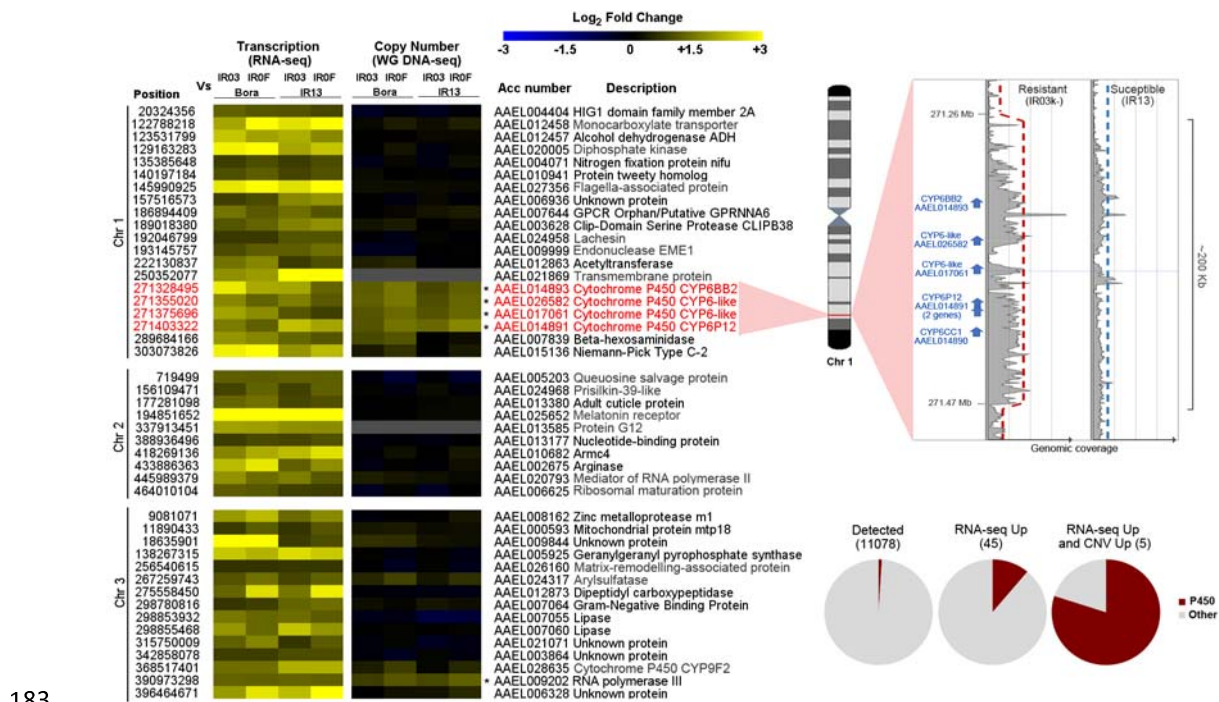
158 As the duplicated P450 locus is located on chromosome 1, which also carries the sex determining  
 159 locus, deltamethrin bioassays were performed on F1 and F2 males and females obtained from both  
 160 'Bora-Bora x IROF' reciprocal crosses in order to investigate the mode of transmission of resistance.  
 161 Such comparative bioassays did not support any significant bias affecting the transmission of  
 162 resistance (Supplementary file 1). For both F1 males and females, mortality levels upon deltamethrin  
 163 exposure were similar in the two reciprocal crosses and intermediate to those of the parental lines,  
 164 indicating the absence of a maternal effect and a semi-dominant phenotype in heterozygotes. Similar

165 and intermediate mortality levels were again observed in F2 males and females, suggesting the lack  
 166 of a sex transmission bias.

167

168 *Overexpression of the duplicated CYP6 gene cluster*

169 RNA-seq was used to identify differentially transcribed genes between the two resistant lines (IRO3  
 170 and IROF), and the two susceptible lines (IR13 and Bora-Bora). Among the 11268 protein-coding  
 171 genes passing our coverage filter (82% of all protein coding genes), 84 genes showed a significant and  
 172 consistent differential transcription level in the four 'resistant Vs susceptible' pairwise comparisons  
 173 (see methods, expression fold change  $\geq 1.5$  and adjusted P value  $\leq 0.0005$ ). The 39 genes under-  
 174 transcribed in resistant lines did not include any gene belonging to any family known to be associated  
 175 with insecticide resistance. Conversely, the 45 genes over-transcribed in resistant lines included eight  
 176 genes belonging to gene families associated with metabolic resistance (**Figure 2** and **Supplementary**  
 177 **file 2**). These included five P450s (*CYP6BB2* AEEL014893, *CYP6-like* AEEL026852, *CYP6-like*  
 178 AEEL017061, *CYP6P12* AEEL014891 and *CYP9F-like* AEEL028635). The four *CYP6* genes showed mean  
 179 fold changes up to 4.0 folds and belong to a cluster of five consecutive *CYP6* genes located at ~271  
 180 Mb on chromosome 1. Among them, *CYP6P12* (AEEL014891) was annotated as a single accession in  
 181 the reference genome while both protein sequence and RNA-seq data support the presence of two  
 182 distinct genes hereafter referred to as *CYP6P12v1* and *CYP6P12v2* when appropriate.



183

184 **Figure 2.** Genes over transcribed in resistant lines and their associated copy number variations. Only the 45 genes found  
 185 significantly over transcribed from RNA-seq are shown ( $FC \geq 1.5$  and corrected P value  $\leq 0.0005$  in all resistant versus  
 186 susceptible pairwise comparisons). Genes also showing an elevated copy number from WG DNA-seq ( $FC \geq 1.5$ ) in all  
 187 pairwise comparisons are indicated with stars. Genomic coordinates (chromosome and start position), accession number  
 188 and description are indicated for all genes. Gene descriptions in grey were obtained from a BlastP against NCBI Refseq.  
 189 Genes in red belong to a single duplicated region on chromosome 1. Pool-seq read coverage profiles of the susceptible IR13  
 190 and the resistant IROF lines around the duplicated locus are shown. Pie charts show the proportion of P450s in each  
 191 dataset.

192

193 Whole genome Pool-seq short read data were then used to identify genes affected by copy number  
 194 variations in association with resistance base on their normalised exonic coverage. This analysis

195 identified 22 genes showing a congruent elevated copy number (CN) in resistant Vs susceptible lines  
196 (FC  $\geq 1.5$  in all 'resistant Vs susceptible' pairwise comparisons). These included seven P450s. One of  
197 them (AAEL009018) was located at ~58.8 Mb on chromosome 1 and was not detected as over-  
198 transcribed from RNA-seq. The six others were located at ~271 Mb on chromosome 1 and included  
199 the five *CYP6*s found over-transcribed in resistant lines (see above) and another *CYP6* (*CYP6CC1*) from  
200 the same gene cluster that was filtered out from RNA-seq analysis due to its low transcription level  
201 (**Figure 2** and **Supplementary file 2**). The over-transcribed CYP9F-like located on chromosome 3  
202 showed a slight increased CN in the IROF line Vs the Bora-Bora line (1.6 fold) but such increased CN  
203 was not confirmed for the three other 'resistant Vs susceptible comparisons' (1.07, 1.4 and 1.2 fold  
204 for IR03/IR13, IROF/IR13 and IR03/Bora respectively). A closer look at the genomic coverage at the  
205 *CYP6* locus on chromosome 1 revealed a ~2 folds increased coverage affecting a region of ~200 Kb  
206 spanning the entire *CYP6* cluster. Such duplication was observed in all resistant Vs susceptible  
207 comparisons. Altogether, these genomic data showed that the deltamethrin resistance phenotype  
208 observed in the resistant lines is associated with the presence of a large duplication on chromosome  
209 1 affecting the transcription level of six clustered *CYP6* genes.

210 Whole genome short reads data confirmed the absence of the three major *kdr* mutations Val410Leu,  
211 Val1016Ile and Phe1534Cys in the IROF resistant line, while another *kdr* mutation (Ile1011Met) was  
212 identified at an exact 0.5 frequency (141/282 short reads supporting the 1011Met allele). Indeed,  
213 both short read and long read data confirmed that this Ile1011Met *kdr* mutation is affected by an  
214 heterogenous genomic duplication (see below and in Martins et al., 2013). Therefore, a 0.5  
215 frequency indicates that the Ile-Met/Ile-Met genotype is fixed in the IROF line.

216

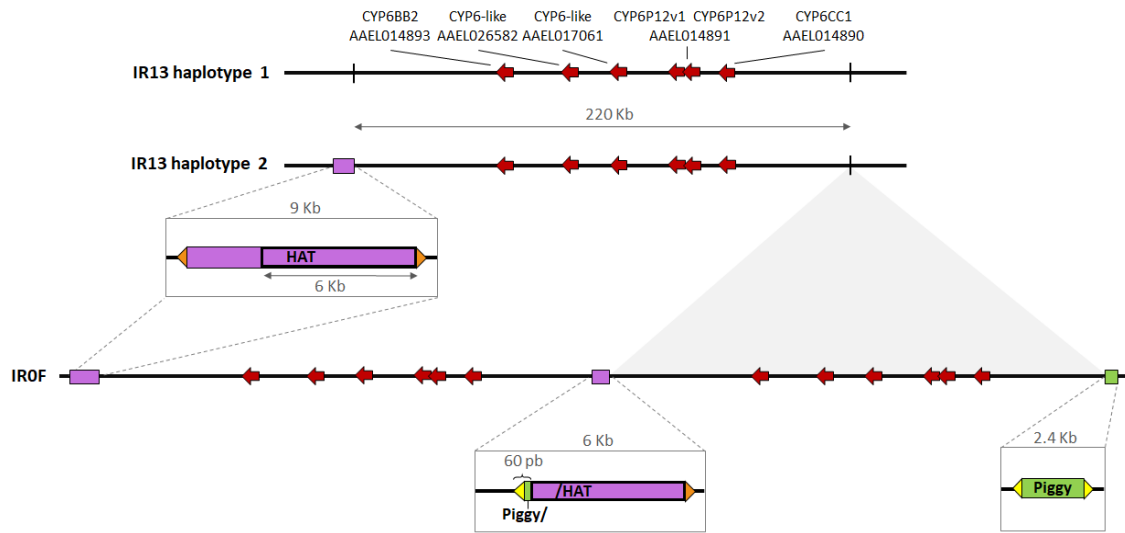
### 217 *Genomic architecture of the duplicated loci*

218 Though not the major aim of the present study, our genomic data allowed characterizing the  
219 architecture of the duplication affecting the Ile1011Met *Kdr* mutation in the IROF line. Both short  
220 read and long read topologies confirmed that the Ile1011Met *kdr* mutation is part of 125 Kb genomic  
221 duplication covering the 21 last coding exons of the VGSC gene AAEL023266 (**Supplementary file 3**).  
222 The breakpoints of this partial gene duplication are located at 315,905,811 bp and 316,030,250 bp on  
223 the reference genome AaegL5. The partial 3' copy carries the wild type allele (1011Ile) while the full-  
224 length copy carries the resistant allele (1011Met). The two copies also differed by their intronic  
225 sequence with the partial copy bearing a B type intron and the full-length copy bearing a A type  
226 intron as previously described (Martins et al., 2013). As expected from an incomplete gene  
227 duplication, RNA-seq data supported the sole expression of the 1011Met allele meaning that the  
228 IROF line (genotype Ile-Met/Ile-Met) express a Met phenotype.

229 The genomic structure of the P450 duplicated region identified on chromosome 1 was further  
230 investigated in light of long reads data obtained from the IR13 susceptible line and the IROF resistant  
231 line. This revealed the presence of a 220.4 Kb duplication in the IROF line, with the two tandem  
232 repeats separated by a 6 Kb insertion (**Figure 3**). The right breakpoint of the duplication (RB) was  
233 found ~50 Kb right to *CYP6CC1* at position 271,472,082 bp, and the left breakpoint (LB) ~77 Kb left to  
234 *CYP6BB2* at 271,251,705 bp. These breakpoints were supported by split reads from both long and  
235 short read data (**Supplementary file 4**). The duplication is flanked by two distinct transposons, each  
236 having its own terminal inverted repeats (TIR): a 2.4 Kb PiggyBac-like transposon on the right (PYL),  
237 and 9 Kb hAT-related transposon on the left (hAT-CYP6). These transposons are described in more  
238 detail in **Supplementary file 5**.

239





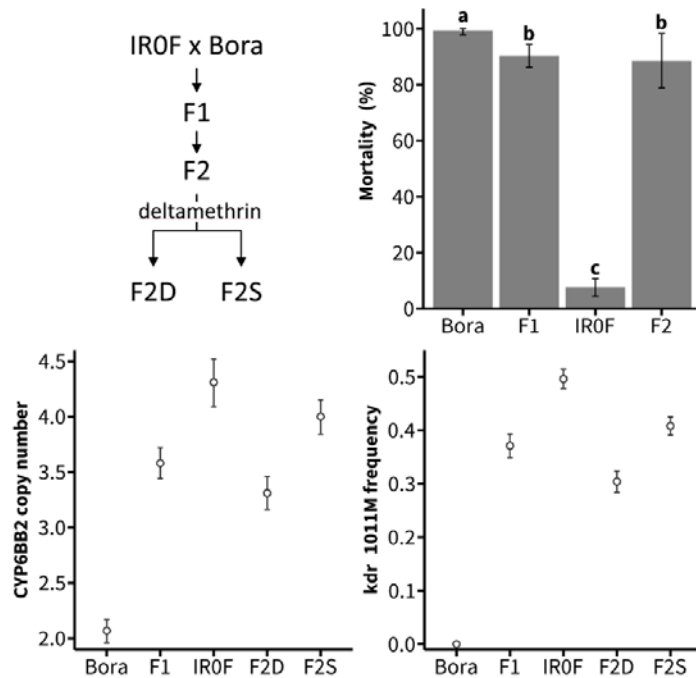
240

241 **Figure 3. Genomic architecture of the duplication.** The topology was deduced from both short and long reads sequencing  
 242 data. The six CYP6 genes carried by the duplication in the resistant lines are represented by red arrows. Regions containing  
 243 full or partial transposable elements are shown in greater detail. Orange and yellow triangles denote the inverted terminal  
 244 repeats from hAT (17 pb) and PiggyBac-like (18 pb) elements respectively. Diagram is not to scale.  
 245

246 The central sequence joining the tandem copies is chimeric, with 60 bp from the left end of PYL  
 247 transposon followed by 6001 bp from the right end of the hAT transposon. This duplication is absent  
 248 from the IR13 susceptible line (no read joining RB and LB sequences and no PYL transposon  
 249 sequence, neither full nor partial at RB). However, the hAT-CYP6 transposon was identified at the LB  
 250 in one IR13 haplotype, much like in the IROF line, while a second haplotype was devoid of hAT  
 251 insertion, much like the reference genome. An excess of tri-allelic SNPs is expected in the duplicated  
 252 region if the two copies have diverged. Pool-seq short read data were then used to compare the  
 253 frequency of tri-allelic loci within the duplication and 100 Kb upward and downward. Among the  
 254 1401 substitutions sites identified within the duplication, five were tri-allelic whereas no such tri-  
 255 allelic variant was identified among the 1334 substitutions identified in the flanking regions. This  
 256 represents a slight but significant enrichment in the duplicated region (Fisher test p value = 0.031).  
 257 These tri-allelic sites were all located within a 11.2 Kb intergenic region between the two *CYP6-like*  
 258 genes AAEL017061 and AAEL014891v1.  
 259

260 *The P450 duplication and the Kdr 1011 mutation are both associated with deltamethrin*  
 261 *survival*

262 The association of the P450 duplication and the *kdr* Ile1011Met mutation with deltamethrin survival  
 263 were investigated in F2 individuals obtained from both 'Bora-Bora x IROF' reciprocal crosses. F2  
 264 females were then exposed to a high dose of deltamethrin (85.5% mortality) before quantifying  
 265 *CYP6BB2* gene copy number and the frequency of the 1011Met *kdr* allele in dead and survivors using  
 266 ddPCR (**Figure 4**). As expected in the presence of a fixed duplication, a 2-fold increase of *CYP6BB2*  
 267 copy number was observed in the IROF line ( $4.31 \pm 0.21$  copies) as compared to Bora-Bora line ( $2.07 \pm$   
 268  $0.10$  copies) while F1 individuals showed an intermediate copy number ( $3.58 \pm 0.14$  copies). In F2  
 269 individuals, *CYP6BB2* copy number was higher in survivors than in dead individuals ( $4.00 \pm 0.16$   
 270 copies versus  $3.31 \pm 0.15$  copies) supporting a genetic linkage between the P450 duplication and  
 271 deltamethrin survival. Insecticide survival was also linked to the *kdr* mutation Ile1011Met on  
 272 chromosome 3. In line with an heterogenous *kdr* duplication, the frequency of the 1011Met allele  
 273 was close to 0.5 in the IROF resistant line (genotype Ile-Met/Ile-Met) and close to 0.33 in F1



individuals (genotype Ile-Met/Ile). In deltamethrin-exposed F2 individuals, the Met allele frequency was higher in survivors than in dead individuals ( $0.41 \pm 0.02$  versus  $0.30 \pm 0.02$ ).

**Figure 4. Genotype-phenotype association study.** Top left panel shows the crossings underlying this experiment. Top right panel shows mortality data obtained by exposing adult females from the IROF and Bora-Bora lines and their F1 and F2 progeny to 0.03% deltamethrin for 1 hour. Mean mortalities  $\pm$  SD 24h after insecticide exposure are shown and distinct letters indicate significant differences (Kruskal-Wallis test followed by post hoc Wilcoxon test with Bonferroni-Holm correction,  $N \geq 5$ ,  $p \leq 0.05$ ). Bottom left and right panels show the copy number of *CYP6BB2* and the frequency of the *kdr* 1011Met allele respectively as inferred by ddPCR from pools of individuals (mean  $\pm$  95% CI, Bora:  $N=19$ , IROF:  $N=23$ , F1:  $N=17$ , F2D:  $N=113$ , F2S:  $N=15$ ). Dead and surviving F2 individuals 24h after insecticide exposure are noted F2D and F2S respectively.

297  
298  
299  
300

### 301 *Multiple CYP genes carried by the P450 duplication may contribute to resistance*

302 The relative importance of the P450s carried by the duplication in deltamethrin survival was then  
303 examined by RNA interference. Direct dsRNA injections in adult females of the IROF line were used to  
304 specifically knock down the five *CYP6* genes showing sufficient expression to be detected by RNA-seq  
305 (*CYP6BB2*, *CYP6-like* AAEL026582, *CYP6-like* AAEL017061, *CYP6P12v1* and *CYP6P12v2*). Such  
306 approach allowed reaching an acceptable silencing specificity and a moderate silencing efficiency  
307 (from 42.2% for AAEL017061 to 69.7% for AAEL026582). Comparative deltamethrin bioassays  
308 performed on dsCYP6-injected mosquitoes and dsGFP-injected controls suggested that the two first  
309 *CYP* gene of the duplicated cluster (*CYP6BB2* and *CYP6-like* AAEL026582) contribute to deltamethrin  
310 survival (see methods and results in **Supplementary file 6**). However, data generated across multiple  
311 injection experiments were not fully conclusive because a high mortality was frequently observed in  
312 dsGFP-injected controls and because the increased mortalities observed in dsCYP6-injected  
313 mosquitoes were relatively low. Such low mortality variations upon dsCYP6 injection were likely due  
314 to the moderate silencing efficiency and the presence of the *kdr* 1011Met allele in the IROF line.  
315

### 316 *The P450 duplication is hardly retained by selection in presence of the Kdr 1011 allele*

317 The co-occurrence of the P450 duplication and the Ile1011Met *kdr* mutation in the IROF resistant line  
318 was taken as an opportunity to compare their responses to deltamethrin selection. Four independent  
319 lines obtained from 'Bora-Bora x IROF' F3 offspring and representing two replicated selection regimes  
320 (selected lines: SelA and SelB, non-selected lines: NSA and NSB) were compared for their resistance  
321 level, *CYP6BB2* copy number and *kdr* 1011Met allele frequency (**Figure 5**).

322

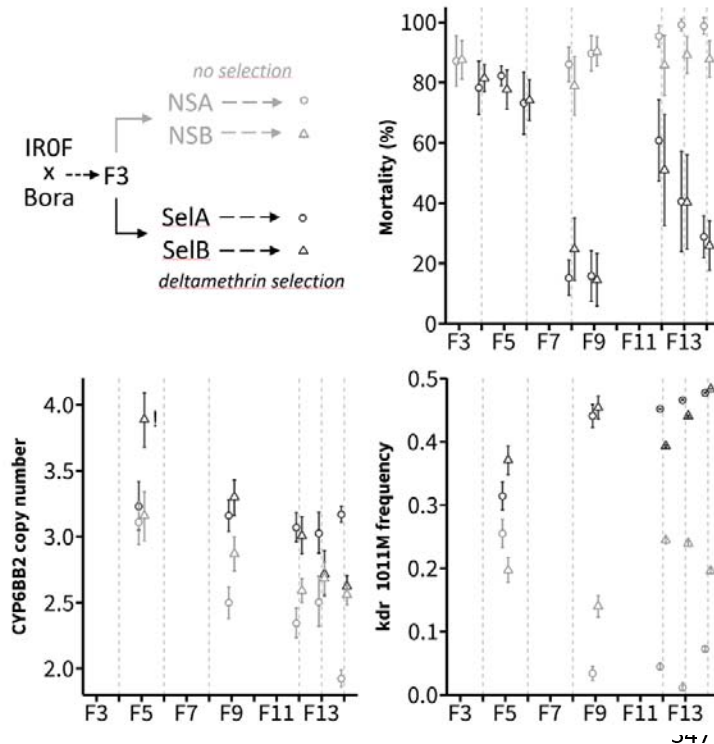


**Figure 5: Response of the P450 duplication and the *kdr* 1011Met allele to deltamethrin selection.** Top left panel shows the crossings underlying this experiment. Top right panel shows the resistance of each line as measured by bioassays on adult females (0.03% deltamethrin for 1h exposure, mean mortality  $\pm$  SD). Bottom left and right panels show *CYP6BB2* copy number and *Kdr* 1011Met frequency respectively as inferred by ddPCR from pools of individuals (mean  $\pm$  95% CI,  $N \geq 30$ ). The SelB *CYP6BB2* copy number data point marked with a '!' was caused by an unexpected sampling error and was therefore excluded from the statistical analysis comparing *CYP6BB2* copy number between Sel and NS lines across generations. Grey dashed lines indicate the generations for which Sel lines were selected with deltamethrin.

348 An increase of deltamethrin resistance was observed for both Sel lines, with mortality dropping from  
 349 ~80% in F4 to less than 20% in F9. Relaxing deltamethrin selection for three successive generations  
 350 (F9 to F11) lead to an increased mortality in both Sel lines, suggesting that the resistance phenotype  
 351 is costly. Though subjected to sampling effects, ddPCR data showed that the *kdr* 1011Met allele was  
 352 rapidly selected by deltamethrin. Its frequency was close to 0.5 in F9 of both Sel lines, supporting the  
 353 near fixation of the Ile-Met duplicated allele. Such increased frequency was not seen in NS lines  
 354 where Met allele frequency decreased to less than 10% in one line and fluctuated under 0.25 in the  
 355 other line. No such strong response to selection was observed for the P450 duplication, with  
 356 *CYP6BB2* copy number showing a gradual decrease through generations in both Sel and NS lines.  
 357 However, *CYP6BB2* mean copy number were significantly higher in Sel lines than in NS lines across  
 358 generations, supporting a higher retention rate of the duplicated allele upon deltamethrin selection  
 359 (Linear Mixed Effect Model,  $p$  value = 0.0088).

360

## 361 Discussion

362 In line with their high probability of occurrence, genomic duplications have been shown to frequently  
 363 contribute to short-term adaptation in various organisms (Kondrashov, 2012). In arthropods facing  
 364 strong selection pressures from insecticides, duplications are known to be adaptive via two distinct  
 365 mechanisms (Bass & Field, 2011). First, heterogeneous duplications affecting key insecticide target  
 366 genes and tethering both susceptible and resistant alleles have been associated with a reduction of  
 367 fitness costs (Labbe et al., 2007). Second, duplications of detoxification genes can contribute  
 368 quantitatively to their over-expression, leading to resistance through increased insecticide  
 369 metabolism (Faucon et al., 2015; Weetman et al., 2018). As opposed to target-site resistance  
 370 mutations that can be easily tracked by PCR in natural populations, the paucity of DNA markers  
 371 underlying metabolic resistance hinders their tracking in the field. In this concern, identifying gene  
 372 duplications associated with metabolic resistance can provide new tools to monitor the dynamics of  
 373 resistance alleles (Cattel et al., 2021).

374

### 375 *The P450 duplication affects a cluster of genes previously associated with resistance*

376 The present study confirmed the occurrence of a large genomic duplication affecting a cluster of six  
377 P450s from the *CYP6* family in *Ae. aegypti* populations from French Guiana. The presence of such a  
378 duplication was previously suspected though the structure of the duplicated loci could not be  
379 resolved from targeted-sequencing data (Faucon et al., 2015). The association of this P450  
380 duplication with deltamethrin resistance was supported by controlled crosses, although the presence  
381 of other resistance alleles limited the association power (Cattel et al., 2020). A duplication  
382 encompassing the *CYP6BB2* gene was also associated with pyrethroid resistance in Lao PDR  
383 (Marcombe et al., 2019). Though gene duplication was not looked for, the over-transcription of *CYP6*  
384 genes from this cluster (e.g. *CYP6BB2*, *CYP6P12* and *CYP6CC1*) was frequently associated with  
385 pyrethroid resistance worldwide (Bariami et al., 2012; Dusfour et al., 2015; Goindin et al., 2017; Kasai  
386 et al., 2014; Marcombe, Poupardin, et al., 2009; Moyes et al., 2017; Reid et al., 2014; Saavedra-  
387 Rodriguez et al., 2012; Seixas et al., 2017). These genes were also found under directional selection in  
388 association with pyrethroid survival in a Mexican resistant line from whole exome SNP data  
389 (Saavedra-Rodriguez et al., 2021). In addition, *CYP6BB2* was also shown capable of metabolising the  
390 pyrethroid permethrin (Kasai et al., 2014). By comparing its copy number and transcriptional level  
391 across different lines, Faucon et al. (2017) suggested that both transcriptional regulation and  
392 genomic duplication contribute to its over-expression in South America. Interestingly, this gene also  
393 responded to selection with the neonicotinoid imidacloprid, suggesting that P450s from this cluster  
394 can be selected by and metabolise other insecticides (Riaz et al., 2013; Zoh et al., 2021).

395 Our attempt to isolate this P450 duplication from other resistance alleles occurring in French Guiana  
396 was partially successful. Indeed, both isofemale lines were naturally deprived from the major  
397 Val1016Iso and Val410Leu *kdr* mutations, and controlled crosses allowed removing the Phe1534Cys  
398 mutation. However, the resulting IROF resistant line carrying the P450 duplication still carried the  
399 Ile1011Met *kdr* mutation as a fixed heterogenous duplication (Ile-Met/Ile-Met genotype, Met/Met  
400 phenotype). There is evidence that this mutation confers some resistance to pyrethroids in the field  
401 (Bregues et al., 2003; Brito et al., 2018; Martins et al., 2009). Nevertheless, the use of the P450  
402 inhibitor PBO showed that the resistance phenotype was still associated with P450-mediated  
403 metabolism. Considering that four of the five P450s over-transcribed in resistant lines belong to the  
404 duplicated locus, the contribution of this P450 duplication to the resistance phenotype is likely.  
405 Studying the mode of transmission of resistance did not allow evidencing any significant sexual  
406 transmission bias potentially associated with resistance. In line with this, this P450 duplication is  
407 located outside of a 210 Mb region of chromosome 1 showing a low recombination rate and a high  
408 genetic differentiation between *Ae. aegypti* males and females (Fontaine et al., 2017).

409

### 410 *Contrasted architectures of the duplications affecting the P450 and the Kdr loci*

411 The presence of two distinct transposons at the P450 duplication breakpoints implies that they have  
412 played an active role in the generation of this genomic event. Transposon-mediated duplication  
413 often arises from ectopic recombination between two homologous transposon copies inserted in the  
414 same orientation at distinct positions of a same chromosome (Baker et al., 1996). However, such an  
415 event would leave a single full-length transposon copy between the two duplicated genomic regions  
416 with no transposon at other breakpoints (Remnant et al., 2013). Here, a more complex scenario must  
417 have taken place because two distinct transposons are flanking the duplication, and because the  
418 sequence joining the two copies is chimeric. A possible scenario involves independent insertion of  
419 the two distinct transposons, then transposition of the hAT into the PiggyBac-like transposon  
420 followed by a deletion event, and finally an ectopic homologous recombination event between the  
421 two duplicated hAT sequences (**Supplementary File 7**). One transposon involved is related to the hAT  
422 superfamily while the other one is distantly related to PiggyBac (see **Supplementary file 5** for more  
423 details), both being cut and paste elements having multiple copies and being active in the *Ae. aegypti*

424 genome (Nene et al., 2007). The divergence of the two tandem copies was supported by the  
425 identification of a few tri-allelic substitution sites within the duplicated region, most likely implying  
426 mutations occurring post-duplication. The few tri-allelic sites observed represent only a fraction of  
427 those, because they imply a pre-duplication mutation at the same position, and because mutations  
428 reverting to the reference allele are not detected as such. Nevertheless, such low divergence rate  
429 between the two copies supports the recent age of this duplication event.

430 In contrast, the genomic duplication affecting the VGSC gene at the *kdr* Ile1011Met locus shows no  
431 remnant of any transposon at breakpoints, suggesting a different genesis than the P450 duplication.  
432 It is likely to be an earlier event, since the copy divergence is much more pronounced, particularly in  
433 intronic regions (Martins et al, 2013). Also, it differs from other heterogenous duplications implicated  
434 so far in insecticide resistance because the incomplete copy carrying the susceptible Ile1011  
435 pseudoallele, does not contribute to gene expression. It therefore cannot modulate the resistance  
436 level provided by the 1011Met allele carried by the full copy, nor its fitness. This contrasts with the  
437 heterogenous duplications affecting the *Ace1* target-site mutation observed in *Culex pipiens sp.* and  
438 *Anopheles gambiae*, where both copies can contribute to the phenotype, thus allowing a reduction  
439 of the fitness cost associated with the resistant allele in absence of insecticide (Djogbenou et al.,  
440 2009; Labbe et al., 2007). In this regard, further investigating the evolutionary origin and dynamics of  
441 this *kdr* heterogenous duplication deserves further attention.

442

#### 443 *The P450 duplication has a limited adaptive value in presence of the Kdr 1011 mutation*

444 The association study performed on F2 individuals supported the association of the P450 duplication  
445 with deltamethrin survival together with the Ile1011Met *kdr* mutation. The association of the  
446 Ile1011Met *kdr* mutation with deltamethrin survival was expected. As the VGSC gene carrying *kdr*  
447 mutations is located on chromosome 3, a genetic linkage with the P450 duplicated loci is excluded.  
448 Therefore, the association of the P450 duplication in F2, following limited recombination events,  
449 implies a resistance locus located on chromosome 1, either the P450 duplication itself or another  
450 genetically linked locus. However, no other known resistance gene was identified in this genomic  
451 region. The relative importance of the different *CYP6* genes carried by the P450 duplication in  
452 deltamethrin survival was investigated through RNA interference. Despite a limited statistical power,  
453 likely due to the presence of the *kdr* Ile1011Met resistance allele and moderate knock down  
454 efficiencies, these data suggest that at least two *CYP6* genes (*CYP6BB2* and AAEL026582) carried by  
455 the duplication may contribute to deltamethrin detoxification.

456 Experimental evolution confirmed the strong positive response of the *kdr* 1011Met allele to selection  
457 with a high dose of deltamethrin. Such experiment also evidenced a gradual decrease of this allele in  
458 absence of insecticide selection, supporting a significant fitness cost as previously shown for other  
459 *kdr* mutations (Rigby et al., 2020; Uemura et al., 2023). The response of the P450 gene duplication to  
460 deltamethrin selection was less clear. A gradual decrease of *CYP6BB2* copy number was observed in  
461 both selected and non-selected lines, even though such decay was slower in the selected lines. Such  
462 result supports a lower adaptive value of the P450 duplication in our experimental conditions. Such  
463 unexpected response may indicate the presence of a significant fitness cost associated with this large  
464 genomic duplication. Indeed, genomic duplications can be detrimental for various reasons (Schrider  
465 et al., 2013): first, gene duplications can alter the gene dosage balance which can lead to metabolic  
466 cost. Second, genomic duplications allow the accumulation of deleterious mutations that are less  
467 cleared off by background selection because of the functional redundancy of duplicated copies.  
468 Third, large duplications can impair recombination locally. In the present case, metabolic costs due to  
469 gene dosage balance and/or a low recombination rate at this locus between the Bora-Bora line (well  
470 adapted to laboratory conditions) and the IROF line (less fitted to our laboratory conditions) may  
471 have impaired the selection of the P450 duplication and favoured the selection of other resistance

472 alleles such as the *kdr* 1011Met mutation. Finally, considering the fitness costs associated with this  
473 *kdr* mutation, its additive cost with the P450 duplication may have prevented their concomitant  
474 selection with the use of a high insecticide dose favouring the selection of the former. Such fitness-  
475 cost balance at two distinct resistance loci may reflect the complex interactions occurring between  
476 resistance alleles *in natura*, leading to distinct adaptive trajectories depending on selection pressures  
477 and demographic effects.

478

## 479 *Conclusions*

480 Following previous work, the present study supports the contribution of this P450 gene duplication in  
481 pyrethroid resistance. However, deciphering its adaptive value *versus* other resistance alleles and its  
482 dynamics in natural mosquito populations deserves further work. The relative importance of the  
483 different *CYP6* genes carried by this duplication in resistance to pyrethroids (and possibly to other  
484 insecticides) also deserves further validation. Despite this incomplete picture, the nature of the  
485 P450s affected by this large genomic duplication and their frequent association with insecticide  
486 resistance call for further studying its evolutionary origin and dynamics in response to xenobiotics. In  
487 this context, though the flanking of the duplication by repeated transposable elements prevented  
488 the design of a specific PCR diagnostic assay targeting the breakpoints, the dual-colour quantitative  
489 TaqMan ddPCR assay we developed (see **Supplementary file 8**) represents a good alternative to track  
490 this resistance allele in natural mosquito populations.

491

## 492 **Methods**

### 493 *Mosquitoes*

494 The *Ae. aegypti* laboratory strain Bora-Bora, fully susceptible to insecticides was used as reference in  
495 the present study. The isofemale lines used in the present study were derived from a field population  
496 collected in 2015 in the Ile Royale (IR) island (5.287° N; 52.590° W) off the coast of French Guiana as  
497 described in Epelboin et al. (2021). Among the isofemale lines isolated from this population, the lines  
498 IR13 and IR03 showed contrasted pyrethroid resistance levels with the IR03 line being highly  
499 resistant and the IR13 line being susceptible as defined by WHO diagnostic dose bioassay (Table 1)  
500 and Epelboin et al. (2021). Both lines were shown to lack the two major voltage-gated sodium  
501 channel *kdr* mutations occurring in this geographical area (Val410Leu and Val1016Ile), yet both  
502 carried the Phe1534Cys mutation at a moderate frequency (Epelboin et al., 2021). The proteomic  
503 profiling of these lines identified multiple cytochrome P450s enriched in the IR03 resistant line as  
504 compared to a susceptible line, supporting the presence of metabolic resistance alleles (Epelboin et  
505 al., 2021). All mosquito lines were maintained under standard laboratory conditions (27 ± 2°C, 70 ±  
506 10 % relative humidity, light/dark cycle 14:10h) and large population size to limit drift effects  
507 (N>1000). Larvae were reared in tap water and fed with hay pellets. Adults were maintained in mesh  
508 cages and fed with a 10% honey solution. Blood feedings were performed on mice.

509

### 510 *Removal of the Phe1534Cys mutation from the IR03 line*

511 In an attempt to isolate metabolic resistance alleles, inter-crosses assisted by genotyping were  
512 performed on the IR03 resistant line to create the IR0F line depleted from the Phe1534Cys *kdr*  
513 mutation. A total of 245 IR03 couples were individualised at the pupal stage in eppendorf tubes  
514 placed in plastic cups covered by a nylon mesh and allowed to emerge and reproduce. The  
515 Phe1534Cys *Kdr* mutation was first searched for from male exuvia for all couples and then from  
516 female exuvia of the 58 couples from which males were negatives for the 1534Cys allele. Genotyping  
517 was performed on qPCR using the High Resolution Melt Curve Analysis method as described in  
518 Saavedra-Rodriguez et al. (2007). The six couples in which both parents were homozygous wild type

519 (Phe-Phe) were transferred to a mesh cage, blood fed and allowed to lay eggs. The absence of the  
520 1534Cys allele in the offspring was confirmed by genotyping 40 individuals of both sexes. Adults were  
521 then exposed to 0.05% deltamethrin and survivors were allowed to freely reproduce to generate the  
522 IROF resistant line. The IROF line was then maintained in standard insectary conditions under  
523 moderate deltamethrin selection pressure (*i.e.* 50% mortality every two generations).

524

### 525 *Deltamethrin bioassays*

526 All bioassays were performed by exposing replicates of 20-25 three days-old non-blood-fed adults to  
527 deltamethrin impregnated filter papers following the standard WHO procedure, with mortality being  
528 recorded 24h after insecticide exposure (WHO, 2022). Different insecticide doses and exposure times  
529 were used according to the nature of the experiment and the mosquito tested (susceptibility status,  
530 sex, use of enzymatic inhibitor or not) in order to keep mortality in the dynamic range and maximise  
531 mortality variations between conditions. The bioassays used for assessing the resistance level of the  
532 different lines presented in Table 1 were performed on females using 10 replicates per line and a  
533 dose of 0.05% deltamethrin for 40 min. The involvement of P450s in the resistance phenotype  
534 presented in Figure 1 was assessed by bioassays on 5 replicates of females exposed or not to 4%  
535 piperonyl butoxide (PBO) for 1h prior to deltamethrin exposure using a dose of 0.03% deltamethrin  
536 for 30 min. Bioassays used to investigate the mode of inheritance of resistance presented in  
537 Supplementary Figure 1 were performed on males and females obtained from the susceptible Bora-  
538 Bora line and the resistant IROF line together with F1 and F2 individuals obtained from each  
539 reciprocal crosses (see below). As males and females naturally show different tolerance to  
540 insecticides and F1/F2 individuals were expected to be more susceptible than IROF individuals,  
541 deltamethrin exposure conditions were accordingly (0.03% deltamethrin for 30 min for females and  
542 0.015% deltamethrin for 25 min). Finally, bioassays used for monitoring the resistance level of the  
543 selected and non-selected lines through the experimental evolution experiment presented in Figure  
544 5 were performed on 5 to 7 replicates per line per generation using a dose of 0.03% deltamethrin for  
545 1h.

546

### 547 *Controlled crosses and association studies*

548 In order to investigate the mode of inheritance of resistance, reciprocal crosses between the fully  
549 susceptible Bora-Bora line and the resistant IROF line were performed (cross A: 'Bora-Bora females x  
550 IROF males' and cross B: 'IROF females x Bora-Bora males'). Crosses were performed with 200 virgin  
551 females and males of each line. The susceptibility of F1 and F2 males and females from each cross  
552 were then compared using deltamethrin bioassays as described above. The association of the P450  
553 duplication with deltamethrin survival was studied in F2 females obtained from both reciprocal  
554 crosses pooled in equal quantities. F2 females were exposed to 0.03% deltamethrin for 1h leading to  
555 88.5% mortality after a 24h recovery time. Dead and surviving females were sampled and stored at -  
556 20°C until molecular analyses. The response of the P450 duplication and the Ile1011Met *ldr*  
557 mutation were further studied across multiple generations using experimental selection. F3 eggs  
558 obtained from both reciprocal crosses were pooled in equal quantity and then randomly split in 4  
559 lines: the first two lines (NSA and NSB) were maintained without insecticide selection, while the two  
560 other lines (SelA and SelB) were selected with deltamethrin. This duplicated line setup was used in  
561 order to control for genetic drift that may occur across generations. Deltamethrin mass selection was  
562 performed prior mating on both virgin males and virgin females (N>1000 for each line) at generations  
563 F4, F6, F8, F12 and F13. A constant dose of deltamethrin was used through the selection process  
564 leading to ~70% mortality in each sex at generation F3 (females: 0.03% for 1h; males: 0.015% for 30  
565 min). The resistance level of each line was monitored at generations F5, F9, F12, F13 and F14 on  
566 females prior to insecticide selection using standard bioassays (see above). Unexposed adult females  
567 from each line were sampled at the same generations and stored at -20°C until molecular analysis.

568

## 569 *RNA-sequencing*

570 Gene transcription levels were compared across the four lines (Bora-Bora, IR13, IR03 and IROF) using  
571 RNA-seq. For each line, four RNA-seq libraries were prepared from distinct batches of 25 calibrated  
572 three-day-old non-blood-fed females not exposed to insecticide. Total RNA was extracted using  
573 TRIzol (Thermo Fisher Scientific) following manufacturer's instructions. RNA samples were then  
574 treated with RNase-free DNase set (Qiagen) to remove gDNA contamination, purified on RNeasy mini  
575 columns (Qiagen) and QC checked using Qubit (Thermo Fisher Scientific) and bioanalyzer (Agilent).  
576 RNA-seq libraries were prepared from 500 ng total RNA using the NEBNext® Ultra™ II directional RNA  
577 library Prep Kit for Illumina (New England Biolabs) following manufacturer's instructions. Briefly,  
578 mRNAs were captured using oligodT magnetic beads and fragmented before being reverse  
579 transcribed using random primers. Double-stranded cDNAs were synthesised, end-repaired, and  
580 adaptors were incorporated at both ends. Libraries were then amplified by PCR for 10 cycles and  
581 purified before QC check using Qubit and Bioanalyzer. Libraries were then sequenced in multiplex as  
582 single 75 bp reads using a NextSeq500 sequencer (Illumina). An average of 51.4 M reads was  
583 generated per library. After unplexing and removing adaptors, sequenced reads from each library  
584 were loaded into Strand NGS V3.2 (Strand Life Science) and mapped to the latest *Ae. aegypti* genome  
585 assembly (Aaeg L5) using the following parameters: min identity = 90%, max gaps = 5%, min aligned  
586 read length = 25, ignore reads with > 5 matches, 3' end read trimming if quality < 20, mismatch  
587 penalty = 4, gap opening penalty = 6, gap extension penalty = 1. Mapped reads were then filtered  
588 based on their quality and alignment score as follows: mean read quality > 25, max N allowed per  
589 read = 5, alignment score ≥ 90, mapping quality ≥ 120, no multiple match allowed, read length ≥ 35.  
590 These filtering steps allowed retaining ~75% of reads. Quantification of transcription levels was  
591 performed on the 13614 protein-coding genes using the DESeq2 method with 1000 iterations  
592 (Anders & Huber, 2010, <https://bioconductor.org/packages/release/bioc/html/DESeq2.html>). Only  
593 the 11268 protein-coding genes showing a normalised expression level ≥ 0.5 (~0.05 RPKM) in all  
594 replicates for all lines were retained for further analysis. Differential gene transcription levels  
595 between each line across all replicates were then computed using a one-way ANOVA followed by a  
596 Tukey post hoc test and p values were corrected using the Benjamini and Hochberg multiple testing  
597 correction (Benjamini & Hochberg, 1995). Genes showing a transcription variation ≥ 1.5 fold (in  
598 either direction) and an adjusted p value ≤ 0.0005 in the four pairwise comparisons between  
599 resistant and susceptible lines (*i.e.* IR03 Vs Bora-Bora, IR03 Vs IR13, IROF Vs Bora-Bora and IROF Vs  
600 IR13), were considered differentially transcribed in association with deltamethrin resistance.  
601

## 602 *Whole genome Pool-sequencing*

603 The genome of the four lines were compared using short read whole genome pool-seq. For each line,  
604 genomic DNA was extracted from two batches of 50 adult females using the PureGene Core Kit A  
605 (Qiagen) and the two gDNA extracts were then pooled in equal proportion into a single sequencing  
606 library. Whole genome sequencing was performed from 200 ng gDNA. Sequencing libraries were  
607 prepared according to the TruSeq DNA Nano Reference guide for Illumina Paired-end Indexed  
608 sequencing (version oct. 2017) with an insert size of 550 bp. Sequencing was performed on a  
609 NextSeq 550 (Illumina) as 150 bp paired-reads. Sequencing depth was adjusted to reach an average  
610 coverage ≥ 80X leading to the sequencing of ~713 M reads per library. Reads obtained from each line  
611 were loaded into Strand NGS V3.2 and mapped to *Ae. aegypti* genome (Aaeg L5) using the following  
612 parameters: min identity = 90%, max gaps = 5%, min aligned read length = 25, ignore reads with > 5  
613 matches, 3' end read trimming if quality < 15, mismatch penalty = 4, gap opening penalty = 6, gap  
614 extension penalty = 1. Mapped reads were then filtered based on their quality and alignment score  
615 as follows: mean read quality > 25, max N allowed per read = 5, alignment score ≥ 90, mapping  
616 quality ≥ 60, no multiple match allowed, read length ≥ 100. Finally, interchromosomal split reads and  
617 PCR duplicates were removed. These filtering steps allowed retaining ~53% of reads.



618 In order to focus on duplication impacting protein expression, gene copy number variation (CNV)  
619 analysis was performed on exons of all protein-coding genes. For each gene, raw coverages were  
620 obtained by dividing the number of reads mapped to all (non-overlapping) exons by total exon  
621 length. Normalised gene coverages were then obtained by dividing raw gene coverages by the total  
622 number of reads passing mapping and quality filters from each sequenced library. In order to limit  
623 false positives in low coverage regions, genes showing a normalised coverage value  $< 1E-8$  in at least  
624 one line were filtered out (12145 genes retained). As for RNA-seq, genes showing a CNV  $\geq 1.5$  fold (in  
625 either direction) in the four pairwise 'resistant vs susceptible' comparisons were considered affected  
626 by CNV in association with resistance.

627 The divergence between the two copies of the P450 duplication was investigated through the  
628 detection of tri-allelic substitution sites in the IROF resistant line. Substitutions were called from reads  
629 mapped within a region encompassing the P450 duplication extended by 100 kb on both sides  
630 (Chr1:271151705 - Chr1:271572082). Only substitutions showing a coverage  $>40$  reads and minimum  
631 allele frequency = 10% were called, allowing the detection of 1401 and 1334 substitution sites within  
632 and outside the duplicated region respectively. Substitution sites were then considered as tri-allelic  
633 if they carried the reference allele together with two distinct variant alleles at the same position,  
634 each showing a frequency  $> 20\%$ .

635

#### 636 *Long read sequencing and de novo assembly of the P450 duplication*

637 The genomic architecture of the duplicated locus was further examined in the duplicated IROF line  
638 versus the non-duplicated IR13 line. Both lines were submitted to long read sequencing using Oxford  
639 Nanopore technology. Genomic DNA was extracted from pools of 75 adult females using the Genra  
640 Puregene Tissue kit (Qiagen) with 3 mL cell lysis buffer. Genomic DNA was quantified using Qubit  
641 DNA Broad Range assay (Qiagen) and quality-checked by agarose gel electrophoresis before adjusting  
642 concentration to 150 ng/ $\mu$ l. Long genomic DNA fragments were selected using the Short Read  
643 Eliminator kit (Circulomics). DNA libraries were prepared using 1  $\mu$ g gDNA with the ligation  
644 sequencing kit SQK-LSK109 kit (Oxford Nanopore) following manufacturer's instructions. Finally, 50  
645 fmoles of the resulting DNA library were loaded on a R9.4.1 MinIon flow cell. Long read sequences  
646 were collected from 2 independent runs of 48 h for each line. Sequencing generated a total of  
647 515K/1017K reads with an average length of 13.5/9.8 Kb, representing 3.4/4.8-fold genome  
648 coverage, for IROF and IR13 lines respectively. Reads were mapped on the AaegL5 reference genome  
649 using Winnowmap (Jain et al., 2022) and alignments were visualised using IGV (Robinson et al.,  
650 2011). Finally, de novo genomes of the IROF and IR13 lines were assembled using both short and long  
651 reads using MaSuRCA (Zimin et al., 2013). This de novo assembly resulted into 17346/ 13160 contigs,  
652 with a median size of 40/55 kb for each line respectively. Transposable elements were identified  
653 using BLAST against the RepBase library (10/12/2021 version).

654

#### 655 *Quantification of the P450 duplication*

656 The detection of the P450 duplication was achieved through the quantification of *CYP6BB2* copy  
657 number by digital droplet PCR (ddPCR). Genomic DNA was extracted from pools of mosquitoes using  
658 the cetyltrimethylammonium bromide (CTAB) method (Collins et al 1987), resuspended in nuclease-  
659 free water and quantified using Qubit DNA Broad Range assay (Qiagen). The duplex ddPCR  
660 quantification assay was based on the co-amplification of two target genes each detected with  
661 specific Taqman probes: the gene *CYP6BB2* (AAEL014893, Fam) was used to quantify the P450  
662 duplication copy number while the gene *CYP4D39* (AAEL007808, Hex) always found as a single copy  
663 in various *Ae. aegypti* lines was used as control for normalisation of gDNA quantities (Faucon et al.,  
664 2015). Before amplification, gDNA samples were digested with XhoI for 15 min at 37°C directly within  
665 the ddPCR reaction mixture. This reaction mixture was partitioned into up to 20,000 nanoliter-sized

666 droplets using the QX200 droplet generator (Bio-Rad) by mixing 70  $\mu$ l of synthetic oil with 20  $\mu$ l PCR  
667 mix. Then, 40 $\mu$ L of the partitioned reaction was amplified for 40 cycles with an annealing  
668 temperature of 60°C (see **Supplementary file 8** for protocol details and primers/probes). After  
669 amplification, the number of positive and negative droplets was quantified for both Fam and Hex  
670 channels using the QX200 droplet reader (Bio-Rad) and the positive/negative ratio was used to  
671 estimate the initial gDNA concentration of each gene assuming a Poisson distribution. After  
672 normalisation for gDNA quantity, *CYP6BB2* copy number were expressed as mean copy number ( $\pm$   
673 95% CI).

674

#### 675 *Quantification of the Ile1011Met kdr mutation frequency*

676 The frequency of the Ile1011Met kdr mutation was quantified on pools of mosquitoes using ddPCR.  
677 Genomic DNA was extracted as described above and digested with XhoI for 15 min at 37°C before  
678 partitioning. The duplex TaqMan reaction mixture contained two amplification primers together with  
679 two Taqman probes labelled with Fam and Hex fluorophores corresponding to the Met and Iso alleles  
680 respectively (see **Supplementary file 8** for protocol and primer/probes details). The duplex reaction  
681 mixture was emulsified as described above and amplified for 40 cycles with an annealing  
682 temperature of 59°C. After droplet reading, the positive/negative ratio obtained for each channel  
683 was visualised as a scatterplot and was used to estimate the frequency of each allele assuming a  
684 Poisson distribution with 95% CI.

685

## 686 **Aknowledgments**

687 We thank the Institut Pasteur de La Guyane for providing the isofemale lines IR03 and IR13. We also  
688 thank Dr. Ademir Jesus Martins from the Fundación Oswaldo Cruz for a critical reading of the  
689 manuscript.

690

## 691 **Conflict of interest disclosure**

692 The authors declare that they comply with the PCI rule of having no financial conflicts of interest in  
693 relation to the content of the article.

694

## 695 **Authors' contributions**

696 JMB and JPD designed the study. TB, CH, JG, JC, MK, LN, TG, FL and JT performed experiments and  
697 analysed data. JF, FB, JV, JMB and JPD supervised data analysis. ID provided biological materials and  
698 data. JMB, JF and JPD acquired the funding. TB, JMB and JPD wrote and revised the paper.

699

## 700 **Data availability**

701 RNA-seq data have been deposited at EBI short read archive (SRA) under accession number E-MTAB-  
702 13325. DNA-seq short and long reads have been deposited at EBI short read archive (SRA) under  
703 accession number E-MTAB-13310.

704

## 705 **Ethical aspects**

706 Mice were kept in the animal facility of the Biology department of the University of Grenoble-Alpes,  
707 approved by the French Ministry of Animal Welfare (agreement no. B 38 421 10 001) and used in  
708 accordance with the laws of the European Union (directive 2010/63/EU). The use of animals for this

709 study was approved by the ComEth Grenoble-C2EA-12 ethics committee mandated by the French  
710 Ministry of Higher Education and Research (MENESR). The study was conducted in accordance with  
711 the ARRIVE guidelines.  
712

### 713 **Funding**

714 This study was funded by the European Union's Horizon 2020 research and innovation program  
715 under the *ZIKAlliance* project [grant agreement no. 734548] and the *Infravec2* project [grant  
716 agreement no. 731060]. MK and TB were respectively supported by mobility fellowships funded by  
717 the European Union's Horizon 2020 research and innovation under the *AIM COST action* [grant  
718 agreement no. CA17108] and the MSCA *INOVEC* project [grant agreement no. 101086257]. Views  
719 and opinions expressed are however those of the authors only and do not necessarily reflect those of  
720 the European Union. Neither the European Union nor the granting authority can be held responsible  
721 for them.

## 722 **Supplementary materials**

723

724 **Supplementary file 1 (.tiff image). Bioassays data from F1 and F2 offspring used to investigate the**  
725 **mode of inheritance of the resistance phenotype.** The reciprocal controlled crosses used to  
726 generate F1 and F2 individuals used for bioassays are indicated. Deltamethrin exposure conditions  
727 were 0.03% deltamethrin for 30 min for females and 0.015% deltamethrin for 25 min for males in  
728 order to account for their inherent lower insecticide tolerance. Mortality rates are indicated as mean  
729  $\pm$  SD. Distinct letters indicate significantly distinct means (Kruskal-Wallis test followed by post hoc  
730 pairwise Wilcoxon test with Bonferroni-Holm correction, N=5,  $p \leq 0.05$ ).

731 **Supplementary file 2 (.xlsx file). RNA-seq and CNV data sets.** All protein coding genes showing a  
732 significant differential transcription (sheet 'RNA-seq') or a significant differential exonic coverage  
733 (sheet 'CNV') are shown. See methods for filtering conditions and thresholds. Gene descriptions  
734 beginning with a # were manually inferred from Blast X result.

735 **Supplementary File 3 (.tiff image). Genomic architecture of the *kdr* locus in the IROF resistant line.**  
736 On chromosome 3, the 3' part of the VGSC gene, including the 21 last exons, is duplicated. Black bars  
737 indicate the position of the coding exons. The duplication is 125 Kb long, and is imperfect: the two  
738 copies, R and R' mostly differing in their intronic sequences. The duplication breakpoints, left (LB)  
739 and right (RB) are located at 315,905,811 bp and 316,030,250 bp on the reference genome AaegL5.  
740 The 1011Met codon is located on the upstream copy (R) and followed by a B type intron. The 1011Ile  
741 codon is on the downstream copy and followed by an A type intron (Martins et al, 2013). RNA-seq  
742 data supported the sole expression of the 1011Met allele.

743 **Supplementary file 4 (.xlsx file). Long reads overlapping the P450 duplication breakpoints.**

744 **Supplementary file 5 (.docx file). Data supporting the identification of the transposable elements**  
745 **flanking the P450 duplication.**

746 **Supplementary file 6 (.docx file). RNA interference experiment.** This document includes detailed  
747 results and methods.

748 **Supplementary file 7 (.tiff image). Proposed evolutionary steps leading to the observed duplication**  
749 **architecture.** Theoretical structures and those inferred from short and long reads data are indicated.  
750 The hAt-like and PiggyBac-like transposons are shown in purple and green respectively. Transposition  
751 events are shown as dashed lines. The second hAt-like transposition event would have created an  
752 incomplete copy of the hAT transposon, either directly or through a posterior deletion.  
753 Recombination events are shown as blue crossed lines. Stars indicates junctions that were confirmed  
754 by short reads data.

755 **Supplementary File 8 (.docx file). Digital droplet PCR assays used to quantify the P450 duplication**  
756 **and the frequency of the Ile1011Met *kdr* mutation.** This document provides all technical details  
757 related these ddPCR assays including amplification primers, TaqMan probes, PCR conditions and data  
758 interpretation.

## 759 References

- 760 Achee, N. L., Grieco, J. P., Vatandoost, H., Seixas, G., Pinto, J., Ching-Ng, L., Martins, A. J.,  
761 Juntarajumnong, W., Corbel, V., Gouagna, C., David, J.-P., Logan, J. G., Orsborne, J., Marois, E.,  
762 Devine, G. J., & Vontas, J. (2019). Alternative strategies for mosquito-borne arbovirus control.  
763 *PLoS Negl Trop Dis*, *13*(1). <https://doi.org/10.1371/journal.pntd.0006822>
- 764 Anders, S., & Huber, W. (2010). Differential expression analysis for sequence count data. *Genome*  
765 *Biology*, *11*(10), R106. <https://doi.org/10.1186/gb-2010-11-10-r106>
- 766 Baker, M. D., Read, L. R., Beatty, B. G., & Ng, P. (1996). Requirements for Ectopic Homologous  
767 Recombination in Mammalian Somatic Cells. *Molecular and Cellular Biology*, *16*(12), 7122-7132.  
768 <https://doi.org/10.1128/MCB.16.12.7122>
- 769 Bariami, V., Jones, C. M., Poupardin, R., Vontas, J., & Ranson, H. (2012). Gene Amplification, ABC  
770 Transporters and Cytochrome P450s: Unraveling the Molecular Basis of Pyrethroid Resistance in  
771 the Dengue Vector, *Aedes aegypti*. *PLoS Negl Trop Dis*, *6*(6).  
772 <https://doi.org/10.1371/journal.pntd.0001692>
- 773 Bass, C., & Field, L. M. (2011). Gene amplification and insecticide resistance. *Pest Management*  
774 *Science*, *67*(8), 886-890. <https://doi.org/10.1002/ps.2189>
- 775 Benjamini, Y., & Hochberg, Y. (1995). Controlling the False Discovery Rate: A Practical and Powerful  
776 Approach to Multiple Testing. *J Royal Stat Soc B*, *57*, 289-300. [https://doi.org/10.1111/j.2517-](https://doi.org/10.1111/j.2517-6161.1995.tb02031.x)  
777 [6161.1995.tb02031.x](https://doi.org/10.1111/j.2517-6161.1995.tb02031.x)
- 778 Brengues, C., Hawkes, N. J., Chandre, F., McCarroll, L., Duchon, S., Guillet, P., Manguin, S., Morgan, J.  
779 C., & Hemingway, J. (2003). Pyrethroid and DDT cross-resistance in *Aedes aegypti* is correlated  
780 with novel mutations in the voltage-gated sodium channel gene. *Med Vet Entomol*, *17*(1), 87-94.  
781 <https://doi.org/10.1046/j.1365-2915.2003.00412.x>
- 782 Brito, L. P., Carrara, L., Freitas, R. M. D., Lima, J. B. P., & Martins, A. J. (2018). Levels of Resistance to  
783 Pyrethroid among Distinct *kdr* Alleles in *Aedes aegypti* Laboratory Lines and Frequency of *kdr*  
784 Alleles in 27 Natural Populations from Rio de Janeiro, Brazil. *BioMed Research International*, *2018*,  
785 [1-10](https://doi.org/10.1155/2018/2410819). <https://doi.org/10.1155/2018/2410819>
- 786 Brown, J. E., Evans, B. R., Zheng, W., Obas, V., Barrera-Martinez, L., Egizi, A., Zhao, H., Caccone, A., &  
787 Powell, J. R. (2014). Human impacts have shaped historical and recent evolution in *Aedes aegypti*,  
788 the dengue and yellow fever mosquito. *Evolution*, *68*(2), 514-525.  
789 <https://doi.org/10.1111/evo.12281>
- 790 Carvalho, V. L., & Long, M. T. (2021). Perspectives on New Vaccines against Arboviruses Using Insect-  
791 Specific Viruses as Platforms. *Vaccines*, *9*(3), 263. <https://doi.org/10.3390/vaccines9030263>
- 792 Cattel, J., Faucon, F., Le Peron, B., Sherpa, S., Monchal, M., Grillet, L., Gaude, T., Laporte, F., Dusfour,  
793 I., Reynaud, S., & David, J. P. (2020). Combining genetic crosses and pool targeted DNA-seq for  
794 untangling genomic variations associated with resistance to multiple insecticides in the mosquito  
795 *Aedes aegypti*. *Evolutionary Applications*, *303*-317. <https://doi.org/10.1111/eva.12867>
- 796 Cattel, J., Haberkorn, C., Laporte, F., Gaude, T., Cumer, T., Renaud, J., Sutherland, I. W., Hertz, J. C.,  
797 Bonneville, J., Arnaud, V., Fustec, B., Boyer, S., Marcombe, S., & David, J. (2021). A genomic  
798 amplification affecting a carboxylesterase gene cluster confers organophosphate resistance in the  
799 mosquito *Aedes aegypti*: From genomic characterization to high-throughput field detection.  
800 *Evolutionary Applications*, *14*(4), 1009-1022. <https://doi.org/10.1111/eva.13177>
- 801 Corbel, V., & N'Guessan, R. (2013). Distribution, Mechanisms, Impact and Management of Insecticide  
802 Resistance in Malaria Vectors: A Pragmatic Review, Anopheles mosquitoes -. *New insights into*  
803 *malaria vectors*. <https://doi.org/10.5772/56117>

- 804 David, J. P., Ismail, H. M., Chandor-Proust, A., & Paine, M. J. I. (2013). Role of cytochrome P450s in  
805 insecticide resistance: Impact on the control of mosquito-borne diseases and use of insecticides  
806 on Earth. *Philosophical Transactions of the Royal Society B-Biological Sciences*, 368(1612).  
807 <https://doi.org/10.1098/rstb.2012.0429>
- 808 Djogbenou, L., Labbe, P., Chandre, F., Pasteur, N., & Weill, M. (2009). Ace-1 duplication in *Anopheles*  
809 *gambiae*: A challenge for malaria control. *Malar J*, 8, 70. [https://doi.org/10.1186/1475-2875-8-](https://doi.org/10.1186/1475-2875-8-70)  
810 70
- 811 Dusfour, I., Thalmensy, V., Gaborit, P., Issaly, J., Carinci, R., & Girod, R. (2011). Multiple insecticide  
812 resistance in *Aedes aegypti* (Diptera: Culicidae) populations compromises the effectiveness of  
813 dengue vector control in French Guiana. *Mem Inst Oswaldo Cruz*, 106(3), 346-352.  
814 <https://doi.org/DOI: 10.1590/s0074-02762011000300015>
- 815 Dusfour, I., Vontas, J., David, J. P., Weetman, D., Fonseca, D. M., Raghavendra, K., Corbel, V.,  
816 Coulibaly, M., Martins, A. J., & Chandre, F. (2019). Management of insecticide resistance in the  
817 major *Aedes* vectors of arboviruses: Advances and challenges. *Plos Neg Trop Dis*, 13(10),  
818 e0007615. <https://doi.org/10.1371/journal.pntd.0007615>
- 819 Dusfour, I., Zorrilla, P., Guidez, A., Issaly, J., Girod, R., Guillaumot, L., Robello, C., & Strode, C. (2015).  
820 Deltamethrin Resistance Mechanisms in *Aedes aegypti* Populations from Three French Overseas  
821 Territories Worldwide. *PLoS Negl Trop Dis*, 9(11), e0004226.  
822 <https://doi.org/10.1371/journal.pntd.0004226>
- 823 Epelboin, Y., Wang, L., Giai Gianetto, Q., Choumet, V., Gaborit, P., Issaly, J., Guidez, A., Douché, T.,  
824 Chaze, T., Matondo, M., & Dusfour, I. (2021). CYP450 core involvement in multiple resistance  
825 strains of *Aedes aegypti* from French Guiana highlighted by proteomics, molecular and  
826 biochemical studies. *PLOS ONE*, 16(1), e0243992. <https://doi.org/10.1371/journal.pone.0243992>
- 827 Faucon, F., Dusfour, I., Gaude, T., Navratil, V., Boyer, F., Chandre, F., Sirisopa, P., Thanispong, K.,  
828 Juntarajumnong, W., Poupardin, R., Chareonviriyaphap, T., Girod, R., Corbel, V., Reynaud, S., &  
829 David, J. P. (2015). Identifying genomic changes associated with insecticide resistance in the  
830 dengue mosquito *Aedes aegypti* by deep targeted sequencing. *Genome research*, 25(9),  
831 1347-1359. <https://doi.org/10.1101/gr.189225.115>
- 832 Faucon, F., Gaude, T., Dusfour, I., Navratil, V., Corbel, V., Juntarajumnong, W., Girod, R., Poupardin,  
833 R., Boyer, F., Reynaud, S., & David, J. P. (2017). In the hunt for genomic markers of metabolic  
834 resistance to pyrethroids in the mosquito *Aedes aegypti*: An integrated next-generation  
835 sequencing approach. *PLoS Negl Trop Dis*, 11(4), e0005526.  
836 <https://doi.org/10.1371/journal.pntd.0005526>
- 837 Feyereisen, R., Dermauw, W., & Van Leeuwen, T. (2015). Genotype to phenotype, the molecular and  
838 physiological dimensions of resistance in arthropods. *Pesticide Biochemistry and Physiology*, 121,  
839 61-77. <https://doi.org/10.1016/j.pestbp.2015.01.004>
- 840 French-Constant, R. H., Daborn, P. J., & Le Goff, G. (2004). The genetics and genomics of insecticide  
841 resistance. *Trends Genet*, 20(3), 163-170. <https://doi.org/10.1016/j.tig.2004.01.003>
- 842 Fontaine, A., Filipović, I., Fansiri, T., Hoffmann, A. A., Cheng, C., Kirkpatrick, M., Rašić, G., &  
843 Lambrechts, L. (2017). Extensive Genetic Differentiation between Homomorphic Sex  
844 Chromosomes in the Mosquito Vector, *Aedes aegypti*. *Genome Biology and Evolution*, 9(9),  
845 2322-2335. <https://doi.org/10.1093/gbe/evx171>
- 846 Garg, H., Mehmetoglu-Gurbuz, T., & Joshi, A. (2020). Virus Like Particles (VLP) as multivalent vaccine  
847 candidate against Chikungunya, Japanese Encephalitis, Yellow Fever and Zika Virus. *Scientific*  
848 *Reports*, 10(1), 4017. <https://doi.org/10.1038/s41598-020-61103-1>

- 849 Goindin, D., Delannay, C., Gelasse, A., Ramdini, C., Gaude, T., Faucon, F., David, J. P., Gustave, J.,  
850 Vega-Rua, A., & Fouque, F. (2017). Levels of insecticide resistance to deltamethrin, malathion, and  
851 temephos, and associated mechanisms in *Aedes aegypti* mosquitoes from the Guadeloupe and  
852 Saint Martin islands (French West Indies). *Infect Dis Poverty*, 6(1), 38.  
853 <https://doi.org/10.1186/s40249-017-0254-x>
- 854 Haddi, K., Tome, H. V. V., Du, Y., Valbon, W. R., Nomura, Y., Martins, G. F., Dong, K., & Oliveira, E. E.  
855 (2017). Detection of a new pyrethroid resistance mutation (V410L) in the sodium channel of  
856 *Aedes aegypti*: A potential challenge for mosquito control. *Scientific Reports*, 7, 46549.  
857 <https://doi.org/10.1038/srep46549>
- 858 Hawkins, N. J., Bass, C., Dixon, A., & Neve, P. (2018). The evolutionary origins of pesticide resistance.  
859 *Biol Rev Camb Philos Soc*. <https://doi.org/10.1111/brv.12440>
- 860 Hemingway, J., Hawkes, N. J., McCarroll, L., & Ranson, H. (2004). The molecular basis of insecticide  
861 resistance in mosquitoes. *Insect Biochemistry and Molecular Biology*, 34(7), 653–665.  
862 <https://doi.org/10.1016/j.ibmb.2004.03.018>
- 863 Hendry, A. P., Farrugia, T. J., & Kinnison, M. T. (2008). Human influences on rates of phenotypic  
864 change in wild animal populations. *Molecular Ecology*, 17(1), 20–29.  
865 <https://doi.org/10.1111/j.1365-294X.2007.03428.x>
- 866 Hendry, A. P., Gotanda, K. M., & Svensson, E. I. (2017). Human influences on evolution, and the  
867 ecological and societal consequences. *Philos Trans R Soc Lond B Biol Sci*, 372(1712).  
868 <https://doi.org/10.1098/rstb.2016.0028>
- 869 Hirata, K., Komagata, O., Itokawa, K., Yamamoto, A., Tomita, T., & Kasai, S. (2014). A single crossing-  
870 over event in voltage-sensitive Na<sup>+</sup> channel genes may cause critical failure of dengue mosquito  
871 control by insecticides. *PLoS Negl Trop Dis*, 8(8), e3085.  
872 <https://doi.org/10.1371/journal.pntd.0003085>
- 873 Jain, C., Rhie, A., Hansen, N. F., Koren, S., & Phillippy, A. M. (2022). Long-read mapping to repetitive  
874 reference sequences using Winnowmap2. *Nature Methods*, 19(6), 705–710.  
875 <https://doi.org/10.1038/s41592-022-01457-8>
- 876 Kasai, S., Itokawa, K., Uemura, N., Takaoka, A., Furutani, S., Maekawa, Y., Kobayashi, D., Imanishi-  
877 Kobayashi, N., Amoa-Bosompem, M., Murota, K., Higa, Y., Kawada, H., Minakawa, N., Cuong, T. C.,  
878 Yen, N. T., Phong, T. V., Keo, S., Kang, K., Miura, K., ... Komagata, O. (2022). Discovery of super-  
879 insecticide-resistant dengue mosquitoes in Asia: Threats of concomitant knockdown resistance  
880 mutations. *Science Advances*, 8(51), eabq7345. <https://doi.org/10.1126/sciadv.abq7345>
- 881 Kasai, S., Komagata, O., Itokawa, K., Shono, T., Ng, L. C., Kobayashi, M., & Tomita, T. (2014).  
882 Mechanisms of pyrethroid resistance in the dengue mosquito vector, *Aedes aegypti*: Target site  
883 insensitivity, penetration, and metabolism. *PLoS Negl Trop Dis*, 8(6), e2948.  
884 <https://doi.org/10.1371/journal.pntd.0002948>
- 885 Kondrashov, F. A. (2012). Gene duplication as a mechanism of genomic adaptation to a changing  
886 environment. *Proceedings. Biological Sciences / The Royal Society*, 279(1749), 5048–5057.  
887 <https://doi.org/10.1098/rspb.2012.1108>
- 888 Kraemer, M. U., Sinka, M. E., Duda, K. A., Mylne, A. Q., Shearer, F. M., Barker, C. M., Moore, C. G.,  
889 Carvalho, R. G., Coelho, G. E., Van Bortel, W., Hendrickx, G., Schaffner, F., Elyazar, I. R., Teng, H.-J.,  
890 Brady, O. J., Messina, J. P., Pigott, D. M., Scott, T. W., Smith, D. L., ... Hay, S. I. (2015). The global  
891 distribution of the arbovirus vectors *Aedes aegypti* and *Ae. Albopictus*. *eLife*, 4, e08347.  
892 <https://doi.org/10.7554/eLife.08347>
- 893 Labbe, P., Berthomieu, A., Berticat, C., Alout, H., Raymond, M., Lenormand, T., & Weill, M. (2007).  
894 Independent duplications of the acetylcholinesterase gene conferring insecticide resistance in the

- 895 mosquito *Culex pipiens*. *Mol Biol Evol*, 24(4), 1056–1067.  
896 <https://doi.org/10.1093/molbev/msm025>
- 897 Li, X. C., Schuler, M. A., & Berenbaum, M. R. (2007). Molecular mechanisms of metabolic resistance  
898 to synthetic and natural xenobiotics. *Annual Review of Entomology*, 52, 231–253.  
899 <https://doi.org/10.1146/annurev.ento.51.110104.151104>
- 900 Liu, N. (2015). Insecticide Resistance in Mosquitoes: Impact, Mechanisms, and Research Directions.  
901 *Annual Review of Entomology*, 60(1), 537–559. [https://doi.org/10.1146/annurev-ento-010814-](https://doi.org/10.1146/annurev-ento-010814-020828)  
902 [020828](https://doi.org/10.1146/annurev-ento-010814-020828)
- 903 Lounibos, L. P. (2002). Invasions by insect vectors of human disease. *Annu Rev Entomol*, 47, 233–266.  
904 <https://doi.org/10.1146/annurev.ento.47.091201.145206>
- 905 Marcombe, S., Carron, A., Darriet, F., Etienne, M., Agnew, P., Tolosa, M., Yp-Tcha, M. M., Lagneau, C.,  
906 Yebakima, A., & Corbel, V. (2009). Reduced efficacy of pyrethroid space sprays for dengue control  
907 in an area of Martinique with pyrethroid resistance. *Am J Trop Med Hyg*, 80(5), 745–751.  
908 <https://doi.org/10.4269/ajtmh.2009.80.745>
- 909 Marcombe, S., Darriet, F., Tolosa, M., Agnew, P., Duchon, S., Etienne, M., Yp Tcha, M. M., Chandre, F.,  
910 Corbel, V., & Yebakima, A. (2011). Pyrethroid resistance reduces the efficacy of space sprays for  
911 dengue control on the island of Martinique (Caribbean). *PLoS Negl Trop Dis*, 5(6), e1202.  
912 <https://doi.org/10.1371/journal.pntd.0001202>
- 913 Marcombe, S., Fustec, B., Cattel, J., Chonephetsarath, S., Thammavong, P., Phommavanh, N., David,  
914 J.-P., Corbel, V., Sutherland, I. W., Hertz, J. C., & Brey, P. T. (2019). Distribution of insecticide  
915 resistance and mechanisms involved in the arbovirus vector *Aedes aegypti* in Laos and implication  
916 for vector control. *PLoS Neglected Tropical Diseases*, 13(12), e0007852.  
917 <https://doi.org/10.1371/journal.pntd.0007852>
- 918 Marcombe, S., Poupardin, R., Darriet, F., Reynaud, S., Bonnet, J., Strode, C., Brengues, C., Yebakima,  
919 A., Ranson, H., Corbel, V., & David, J.-P. (2009). Exploring the molecular basis of insecticide  
920 resistance in the dengue vector *Aedes aegypti*: A case study in Martinique Island (French West  
921 Indies). *BMC Genomics*, 10. <https://doi.org/10.1186/1471-2164-10-494>
- 922 Martins, A. J., Brito, L. P., Linss, J. G., Rivas, G. B., Machado, R., Bruno, R. V., Lima, J. B., Valle, D., &  
923 Peixoto, A. A. (2013). Evidence for gene duplication in the voltage-gated sodium channel gene of  
924 *Aedes aegypti*. *Evolution, Medicine, and Public Health*, 2013(1), 148–160.  
925 <https://doi.org/10.1093/emph/eot012>
- 926 Martins, A. J., Lins, R. M., Linss, J. G., Peixoto, A. A., & Valle, D. (2009). Voltage-gated sodium channel  
927 polymorphism and metabolic resistance in pyrethroid-resistant *Aedes aegypti* from Brazil. *Am J*  
928 *Trop Med Hyg*, 81(1), 108–115. <https://doi.org/10.4269/ajtmh.2009.81.108>
- 929 Melo Costa, M., Campos, K. B., Brito, L. P., Roux, E., Melo Rodovalho, C., Bellinato, D. F., Lima, J. B. P.,  
930 & Martins, A. J. (2020). Kdr genotyping in *Aedes aegypti* from Brazil on a nation-wide scale from  
931 2017 to 2018. *Scientific Reports*, 10(1), 13267. <https://doi.org/10.1038/s41598-020-70029-7>
- 932 Moyes, C. L., Vontas, J., Martins, A. J., Ng, L. C., Koou, S. Y., Dusfour, I., Raghavendra, K., Pinto, J.,  
933 Corbel, V., David, J. P., & Weetman, D. (2017). Contemporary status of insecticide resistance in  
934 the major *Aedes* vectors of arboviruses infecting humans. *PLoS Negl Trop Dis*, 11(7), e0005625.  
935 <https://doi.org/10.1371/journal.pntd.0005625>
- 936 Nene, V., Wortman, J. R., Lawson, D., Haas, B., Kodira, C., Tu, Z. J., Loftus, B., Xi, Z., Megy, K.,  
937 Grabherr, M., Ren, Q., Zdobnov, E. M., Lobo, N. F., Campbell, K. S., Brown, S. E., Bonaldo, M. F.,  
938 Zhu, J., Sinkins, S. P., Hogenkamp, D. G., ... Severson, D. W. (2007). Genome sequence of *Aedes*  
939 *aegypti*, a major arbovirus vector. *Science*, 316(5832), 1718–1723.  
940 <https://doi.org/10.1126/science.1138878>



- 941 Orr, H. A. (2005). The genetic theory of adaptation: A brief history. *Nat Rev Genet*, *6*(2), 119–127.  
942 <https://doi.org/10.1038/nrg1523>
- 943 Palumbi, S. R. (2001). Humans as the world's greatest evolutionary force. *Science*, *293*(5536),  
944 1786–1790. <https://doi.org/10.1126/science.293.5536.1786>
- 945 Reid, W. R., Thornton, A., Pridgeon, J. W., Becnel, J. J., Tang, F., Estep, A., Clark, G. G., Allan, S., & Liu,  
946 N. (2014). Transcriptional Analysis of Four Family 4 P450s in a Puerto Rico Strain of *Aedes aegypti*  
947 (Diptera: Culicidae) Compared With an Orlando Strain and Their Possible Functional Roles in  
948 Permethrin Resistance. *Journal of Medical Entomology*, *51*(3), 605–615.  
949 <https://doi.org/10.1603/ME13228>
- 950 Remnant, E. J., Good, R. T., Schmidt, J. M., Lumb, C., Robin, C., Daborn, P. J., & Batterham, P. (2013).  
951 Gene duplication in the major insecticide target site, *Rdl*, in *Drosophila melanogaster*.  
952 *Proceedings of the National Academy of Sciences*, *110*(36), 14705–14710.  
953 <https://doi.org/10.1073/pnas.1311341110>
- 954 Riaz, M. A., Chandor-Proust, A., Dauphin-Villemant, C., Poupardin, R., Jones, C. M., Strode, C., Regent-  
955 Kloeckner, M., David, J.-P., & Reynaud, S. (2013). Molecular mechanisms associated with  
956 increased tolerance to the neonicotinoid insecticide imidacloprid in the dengue vector *Aedes*  
957 *aegypti*. *Aquatic Toxicology*, *126*, 326–337. <https://doi.org/10.1016/j.aquatox.2012.09.010>
- 958 Rigby, L. M., Rašić, G., Peatey, C. L., Hugo, L. E., Beebe, N. W., & Devine, G. J. (2020). Identifying the  
959 fitness costs of a pyrethroid-resistant genotype in the major arboviral vector *Aedes aegypti*.  
960 *Parasites & Vectors*, *13*(1), 358. <https://doi.org/10.1186/s13071-020-04238-4>
- 961 Robinson, J. T., Thorvaldsdóttir, H., Winckler, W., Guttman, M., Lander, E. S., Getz, G., & Mesirov, J. P.  
962 (2011). Integrative genomics viewer. *Nature Biotechnology*, *29*(1), 24–26.  
963 <https://doi.org/10.1038/nbt.1754>
- 964 Saavedra-Rodriguez, K., Campbell, C. L., Lozano, S., Penilla-Navarro, P., Lopez-Solis, A., Solis-Santoyo,  
965 F., Rodriguez, A. D., Perera, R., & Black Iv, W. C. (2021). Permethrin resistance in *Aedes aegypti*:  
966 Genomic variants that confer knockdown resistance, recovery, and death. *PLOS Genetics*, *17*(6),  
967 e1009606. <https://doi.org/10.1371/journal.pgen.1009606>
- 968 Saavedra-Rodriguez, K., Suarez, A. F., Salas, I. F., Strode, C., Ranson, H., Hemingway, J., & Black, W. C.  
969 th. (2012). Transcription of detoxification genes after permethrin selection in the mosquito *Aedes*  
970 *aegypti*. *Insect Mol Biol*, *21*(1), 61–77. <https://doi.org/10.1111/j.1365-2583.2011.01113.x>
- 971 Saavedra-Rodriguez, K., Urdaneta-Marquez, L., Rajatileka, S., Moulton, M., Flores, A. E., Fernandez-  
972 Salas, I., Bisset, J., Rodriguez, M., McCall, P. J., Donnelly, M. J., Ranson, H., Hemingway, J., & Black,  
973 W. C. (2007). A mutation in the voltage-gated sodium channel gene associated with pyrethroid  
974 resistance in Latin American *Aedes aegypti*. *Insect Molecular Biology*, *16*(6), 785–798.  
975 <https://doi.org/doi:10.1111/j.1365-2583.2007.00774.x>
- 976 Schrider, D. R., Houle, D., Lynch, M., & Hahn, M. W. (2013). Rates and Genomic Consequences of  
977 Spontaneous Mutational Events in *Drosophila melanogaster*. *Genetics*, *194*(4), 937–954.  
978 <https://doi.org/10.1534/genetics.113.151670>
- 979 Seixas, G., Grigoraki, L., Weetman, D., Vicente, J. L., Silva, A. C., Pinto, J., Vontas, J., & Sousa, C. A.  
980 (2017). Insecticide resistance is mediated by multiple mechanisms in recently introduced *Aedes*  
981 *aegypti* from Madeira Island (Portugal). *PLoS Negl Trop Dis*, *11*(7), e0005799.  
982 <https://doi.org/10.1371/journal.pntd.0005799>
- 983 Silva, J. V. J., Lopes, T. R. R., Oliveira-Filho, E. F. D., Oliveira, R. A. S., Durães-Carvalho, R., & Gil, L. H. V.  
984 G. (2018). Current status, challenges and perspectives in the development of vaccines against  
985 yellow fever, dengue, Zika and chikungunya viruses. *Acta Tropica*, *182*, 257–263.  
986 <https://doi.org/10.1016/j.actatropica.2018.03.009>

- 987 Smith, L. B., Kasai, S., & Scott, J. G. (2016). Pyrethroid resistance in *Aedes aegypti* and *Aedes*  
988 *albopictus*: Important mosquito vectors of human diseases. *Pesticide Biochemistry and*  
989 *Physiology*, 133, 1–12. <https://doi.org/10.1016/j.pestbp.2016.03.005>
- 990 Uemura, N., Furutani, S., Tomita, T., Itokawa, K., Komagata, O., & Kasai, S. (2023). Concomitant  
991 knockdown resistance allele, L982W + F1534C, in *Aedes aegypti* has the potential to impose  
992 fitness costs without selection pressure. *Pesticide Biochemistry and Physiology*, 193, 105422.  
993 <https://doi.org/10.1016/j.pestbp.2023.105422>
- 994 Valle, D., Bellinato, D. F., Viana-Medeiros, P. F., Lima, J. B. P., & Martins Junior, A. D. J. (2019).  
995 Resistance to temephos and deltamethrin in *Aedes aegypti* from Brazil between 1985 and 2017.  
996 *Memórias Do Instituto Oswaldo Cruz*, 114, e180544. <https://doi.org/10.1590/0074-02760180544>
- 997 Weetman, D., Djogbenou, L. S., & Lucas, E. (2018). Copy number variation (CNV) and insecticide  
998 resistance in mosquitoes: Evolving knowledge or an evolving problem? *Curr Opin Insect Sci*, 27,  
999 82–88. <https://doi.org/10.1016/j.cois.2018.04.005>
- 1000 WHO. (2022). *Standard operating procedure for testing insecticide susceptibility of adult mosquitoes*  
1001 *in WHO tube tests. SOP version: WHO Tube test/01/14*. World Health Organization.  
1002 <https://iris.who.int/bitstream/handle/10665/352316/9789240043831-eng.pdf?sequence=1>
- 1003 Yanola, J., Somboon, P., Walton, C., Nachaiwieng, W., Somwang, P., & Prapanthadara, L. A. (2011).  
1004 High-throughput assays for detection of the F1534C mutation in the voltage-gated sodium  
1005 channel gene in permethrin-resistant *Aedes aegypti* and the distribution of this mutation  
1006 throughout Thailand. *Trop Med Int Health*, 16(4), 501–509. [https://doi.org/10.1111/j.1365-](https://doi.org/10.1111/j.1365-3156.2011.02725.x)  
1007 [3156.2011.02725.x](https://doi.org/10.1111/j.1365-3156.2011.02725.x)
- 1008 Zimin, A. V., Marçais, G., Puiu, D., Roberts, M., Salzberg, S. L., & Yorke, J. A. (2013). The MaSuRCA  
1009 genome assembler. *Bioinformatics*, 29(21), 2669–2677.  
1010 <https://doi.org/10.1093/bioinformatics/btt476>
- 1011 Zoh, M. G., Gaude, T., Prud'homme, S. M., Riaz, M. A., David, J.-P., & Reynaud, S. (2021). Molecular  
1012 bases of P450-mediated resistance to the neonicotinoid insecticide imidacloprid in the mosquito  
1013 *Ae. Aegypti*. *Aquatic Toxicology*, 236, 105860. <https://doi.org/10.1016/j.aquatox.2021.105860>
- 1014